International Journal of General Medicine

Dovepress
open access to scientific and medical research

Open Access Full Text Article

ORIGINAL RESEARCH

RETRACTED ARTICLE: MicroRNA-21 Contributes to Cutaneous Squamous Cell Carcinoma Progression via Mediating TIMP3/PI3K/AKT Signaling Axis

This article was published in the following Dove Press journal:
International Journal of General Medicine

Shuhong Yin
Xiuying Lin

Department of Dermatology, The Third Affiliated Hospital of Qiqihar Medical University, Qiqihar, Heilongjiang, 161000, People's Republic of China

Background: Though the therapeutic potentials of microRNAs (miRNAs) are extensively explored in cutaneous squamous cell carcinoma (CSCC), the concrete function of miR-21 in this disorder has not been thoroughly comprehended. Therein, this work is launched to clarify the miR-21-pivoted mechanism in CSCC from the perspective of tissue inhibitor of metalloproteinases-3 (TIMP3) and phosphatidylinositol 3-kinase (PI3K)/protein kinase B (AKT) pathway.

Methods: Microarray-based analysis was utilized to screen out miR-21 with the most up-regulated expression in CSCC tissues. The relation between miR-21 and TIMP3 expression in tissues, and the overall survival of CSCC patients was evaluated. Loss-of-function assays were performed in cells to explore the independent and combined functions of miR-21 and TIMP3 in CSCC cell progression. Mice were injected with miR-21 inhibitor or TIMP3 si for identifying their roles in tumor formation and liver metastasis. The mechanism among miR-21, TIMP3 and PI3K/AKT pathway was interpreted.

Results: MiR-21 was up-regulated while TIMP3 was down-regulated in CSCC tissues, which were connected with unsatisfactory survival of patients. Down-regulating miR-21 inhibited CSCC cell progression and retarded CSCC tumor formation and metastasis in mice. Silencing of TIMP3 reversed the effects of miR-21 down-regulation on CSCC progression. Besides, down-regulating miR-21 inhibited PI3K/AKT pathway activation in CSCC cells via mediating TIMP3.

Conclusion: It is elucidated that miR-21 depletion impedes CSCC cell invasion and metastasis via enhancing TIMP3 and suppressing PI3K/AKT pathway activation.

Keywords: cutaneous squamous cell carcinoma, microRNA-21, tissue inhibitor of metalloproteinases-3, phosphatidylinositol 3-kinase/protein kinase B pathway, metastasis

Introduction

Cutaneous squamous cell carcinoma (CSCC) is the second most overwhelming non-melanoma skin cancer.[1] The incidence of CSCC is rising with high potential morbidity and mortality, especially in the elderly and immunocompromised people.[2] As to CSCC management in different situations, surgery is recommended for elderly patients with well-differentiated tumors, adjuvant radiation therapy for incomplete resection, radical dissection for patients with positive lymph nodes, while PD-1 inhibitor for advanced CSCC.[3] However, during the period of treatment, recurrence commonly happens in CSCC.[4] Concerning the severity and complexity of this disease, the need for effective agents is still a major task.

Correspondence: Xiuying Lin
Tel/Fax +86-452-2697320
Email xiuyinglin011602@163.com

As a component of microRNA (miRNA), miR-21 has been discussed to own diagnostic, therapeutic and prognostic effects on cutaneous melanoma and CSCC.[5] miRNAs are involved in the initiation, migration, invasion, and chemoresistance in CSCC, and modulate the cellular responses by acting as anti-tumor factors.[6] The significance of miR-21 overexpression in CSCC tumorigenesis has been evaluated in multiple studies. Clinically and experimentally, the resistant CSCC is characterized by elevated miR-21 in patients and mice.[7] Mechanistically, miR-21 has been revealed to be induced in invasive CSCC, harboring diagnostic values.[8] Furthermore, miR-21 has been identified as a pro-oncogene in CSCC and it is overexpressed in CSCC.[9] The binding relationship between miR-21 and tissue inhibitor of metalloproteinases-3 (TIMP3) has been highlighted in cervical cancer.[10] TIMP3, an extracellular matrix-bound protein has been documented to participate in skin cancers.[11] As documented in a study, it is presented that TIMP3 is down-regulated in melanoma progression and it is a negative regulator for cell migration and invasion, as well as anoikis resistance.[12] In addition, there is a study specifically indicating that TIMP3 expression is closely related to angiogenesis in malignant melanoma.[11] miR-21 is clarified to mediate TIMP3, and miR-21 overexpression results in a reduction in TIMP3 expression, thereafter enhancing melanoma cell invasion.[13] However, how their interaction functions in CSCC remain undetermined. Intriguingly, dual-luciferase reporter gene assay in the present study identified the direct binding relationship between miR-21 and TIMP3. Furthermore, phosphatidylinositol 3-kinase (PI3K)/protein kinase B (AKT) pathway has been evidenced to be involved in the pathogenesis of CSCC.[14] Notably, another study has proved that the PI3K/AKT serves as a promotor in CSCC cell growth and development.

On top of that, the combined interplay of miR-21, TIMP3 and PI3K/AKT pathway in CSCC is lack of explorations. Therefore, this work is projected to decode the functions of miR-21/TIMP3/PI3K/AKT pathway axis in CSCC.

Materials and Methods

Clinical Data

Tumor tissues and adjacent tissues were collected from 56 CSCC patients (35 male and 21 female) admitted to the Third Affiliated Hospital of Qiqihar Medical University from June 2013 to June 2016. This study was explicitly approved by the Ethics Committee of the Third Affiliated Hospital of Qiqihar Medical University which followed principles in the Declaration of Helsinki. Written informed consents were obtained from all participants. The tissue specimens were preserved in liquid nitrogen at −80°C. SCC Borders Pathological Classification had clarified CSCC into stage I (well-differentiated) with 0–5% undifferentiated cells, stages II–III (moderately differentiated) with 25–75% undifferentiated cells and stage IV (poorly differentiated) with 75–100% undifferentiated cells. In line with the criteria, 39 cases were well-differentiated, 15 cases were moderately differentiated, and 2 cases were poorly differentiated. The detail information of patients is listed in Table 1.

Microarray-Based Analysis

The tumor and adjacent tissue specimens from CSCC patients were ground with liquid nitrogen and supplemented with Trizol reagent (Thermo Fisher Scientific, Waltham, MA, USA) for total RAN extraction. The RNA purity and integrity were detected by an ultraviolet spectrophotometer and formaldehyde denaturation agarose gel. miRCURY™ Array Power Labeling Kit (Exiqon,

Table 1 Clinicopathological Data of CSCC (n = 56)

Clinical Outcome	Number
Gender (%)	
Male	35 (62.50%)
Female	21 (37.50%)
Age (Years, mean, SE)	
> 50	44 (78.57%)
≤ 50	12 (21.43%)
Tumor size (cm)	
> 3	11 (19.64%)
≤ 3	45 (80.36%)
Histologic cell type	
Well differentiated	39 (69.64%)
Moderately differentiated	15 (26.78%)
Poorly differentiated	2 (3.58%)
Lymph node metastasis	
Absent	52 (92.86%)
Present	4(7.14%)
Venous invasion	
Absent	2 (3.58%)
Present	54 (96.42%)

Abbreviations: CSCC, cutaneous squamous cell carcinoma; SE, standard error.

Copenhagen, Denmark) was thawed on ice. Total RNA (1 μg) was dissolved in ddH_2O (3 μL), incubated with 0.5 μL calf intestinal phosphatase (CIP) buffer at 37°C for 30 min and 0.5 μL CIP and denatured at 95°C for 15 s. Then, the samples were reacted with 3 μL labeling buffer, 1.5 μL Hy3 marker, 2 μL dimethyl sulfoxide and 2 μL marker enzyme on ice in the dark for 1 h at 16°C and incubated at 65°C for 15 min. The labeled RAN (125 μL) was incubated with 90 μL 2 × hybridization buffer and 77.5 μL nuclease-free buffer at 95°C in the dark for 2 min. After hybridization with 180 μL hybridization sample, Axon GenePix 4000B Microarray scanner (Molecular Devices, CA, USA) and GenePix pro V6.0 software were utilized for scanning and analysis. Clustering heatmap was drawn with the ratio of miRNA fluorescence >2 and $p < 0.01$ in CSCC and adjacent tissues.

Reverse Transcription Quantitative Polymerase Chain Reaction (RT-qPCR)

Total RNA extraction from tumor tissues and adjacent tissues and cells were implemented by Trizol reagent (Thermo Fisher Scientific). mRNA reverse transcription into complementary DNA (cDNA) was conducted by a Revert Aid First Strand cDNA Synthesis kit (Thermo Fisher Scientific). Glyceraldehyde-3-phosphate dehydrogenase (GAPDH) and U6 were selected as internal controls. The primer sequences were as follows: miR-21: forward: 5′-GAAAGC-CTG ACAGCTATCGT-3′, reverse: 5′-CGTCGAGAAGACGC ACC-3′. TIMP3: forward: 5′-AAATATGCCACGCTTCA CGA-3′, reverse: 5′-CTACAGTCTGTTGTCTGCTGCTT TT-3′. GAPDH: forward: 5′-TGGATTTCCATTGAT GACAAG-3′, reverse: 5′-ATTCCACCCTTGGCAAATTC -3′. U6: forward: 5′-CGCTTCGGCAGCACATATAC-3′, reverse: 5′-AAATATGCACGCTTCACGA-3′.

Cell Culture and Transfection

CSCC cell lines HSC-1 (JCRB Cell Bank, Osaka, Japan) and A431 (ATCC, VA, USA), human immortalized keratinocytes HaCaT (Cell Lines Service, Eppelheim, Germany) and human embryo kidney epithelial cell HEK293T (ATCC) were cultured in Dulbecco's modified Eagle's medium (DMEM, Thermo Fisher Scientific) supplemented with 10% fetal bovine serum (FBS), 100 μg/mL streptomycin and 100 units/mL penicillin (Sangon, Shanghai, China). MiR-21 inhibitor, si-TIMP3 and the corresponding negative controls (NCs) were synthesized by Genepharma (Shanghai, China). pcDNA 3.1 (Addgene, Cambridge, MA, USA) was adopted to construct low expression vectors. Lipofectamine 3000 was mixed with DNA at 1:1 in Opti-
MEM and added into cells for transfection. At 2 days post-transfection, the cells were analyzed.

Colony Formation Assay

Cells were transfected with low expression vectors and incubated to stable growth. Detached by 0.25% trypsin, cells (5×10^3) were seeded in a 6-well plate containing 1 mL medium, with the medium renewed every 3 days. After a 10-day culture, colonies were visible, and the cells were fixed with 5 mL methanol and stained with 0.5% crystal violet solution. The number of colonies (>10 cells) was calculated, and the rate of colony formation = number of colonies/number of seeded cells × 100%.

5-Ethynyl-2′-Deoxyuridine (EdU) Assay

Cells were detached and seeded at 1×10^6 cells/mL. Cell proliferation was tested by EdU Proliferation Assay Kits (Abcam, San Francisco, USA). Cells were fixed in pre-cool 4% formaldehyde (50 μL) and incubated with 1 μM EdU solution, following staining by 4′6-diamidino-2-phenylindole (Beyotime, Shanghai, China) and observation for the EdU-positive cells under a Leica TCS SPE confocal laser scanning microscope (Leica, IL, USA).

Scratch Test

Seeded in a 6-well plate, cells (1×10^6) were supplemented with medium and cultured to 90% confluence. Scratches were made by a 200-mL pipette, and cell debris were washed with phosphate-buffered saline. Incubated for 5 hours, cells were observed under an inverted microscope (Eclipse Ti, Nikon, Tokyo, Japan) in 5 fields of view. Cell migration ability was detected by wound healing distance.

Transwell Assay

Suspended in 100 μL DMEM to reach 1×10^5 cells/mL, cells were seeded into the apical Transwell chamber with 8-μM pore size and added with Matrigel (Corning, NY, USA). DMEM (200 μL) containing 15% FBS was added to the basolateral Transwell chamber. Following a 24-hour incubation, the cells in the apical chamber were wiped, and those in the basolateral chamber were fixed in 4% paraformaldehyde, stained with 0.5% crystal violet solution and observed under an inverted microscope (Eclipse Ti, Nikon) in 5 five fields of view. Cell invasion was

detected by the number of cells infiltrating to the basolateral chamber.

Flow Cytometry

Cells were seeded in 24-well plates at 1 × 10^5 cells/well and cultured in 10% FBS-DMEM. For apoptosis analysis, cells were trypsinized, centrifuged at 120 g, resuspended in 100 μL 1 × binding buffer and subjected to an Annexin V-fluorescein isothiocyanate/propidium iodide (PI) apoptosis detection kit (Solarbio, Beijing, China). For cell cycle distribution analysis, cells were detached with trypsin (Thermo Fisher Scientific), fixed with 80% ethanol and incubated with 0.25 mg/mL Ribonuclease A (Sigma-Aldrich, Merck KGaA) and 20 μg/mL PI (Roche Applied Science, Mannheim, Germany). Subsequently, a CytoFLEX flow cytometer (Beckman Coulter, Inc., Chaska, MN, USA) was utilized for cell detection, and the cell apoptosis rate and cell cycle distribution were analyzed by CellQuest software (BD Bioscience, San Jose, CA, USA).

Tumor Xenografts in Nude Mice

BALB/c mice of 6–8 weeks (Beijing Vital River Laboratory Animal Technology Co., Ltd., Beijing, China) were injected with 1 × 10^7 cells in 0.2 mL cell suspension at the flank to establish stable CSCC models. The tumor volume was measured every 7 days. At 28 days post-injection, mice were euthanized by intraperitoneal injection of 1% sodium pentobarbital (150 mg/kg). The tumors were weighed. In the metastasis experiment, 1 × 10^7 cells in 0.2 mL cell suspension were injected into mice through the tail vein. After 45 days, mice were euthanized by intraperitoneal injection of 1% sodium pentobarbital (150 mg/kg) for liver metastasis analysis. All the experiments were carried out as per the ARRIVE guidelines and following the National Institutes of Health guide for the care and use of Laboratory animals (revised 1978), and under the approval of the Ethics Committee of the Third Affiliated Hospital of Qiqihar Medical University.

Hematoxylin-Eosin (HE) Staining

The mouse liver tissues were fixed with 4% paraformaldehyde overnight, embedded, sectioned and stained. Dewaxed in xylene, the sections were soaked in gradient alcohol, stained with hematoxylin staining solution (Solarbio) for 5 min and differentiated with 1% hydrochloric acid for 3 s. Following that, the sections were stained by 5% eosin stain (Solarbio) for 3 min, dehydrated and sealed in neutral gum. The sections were observed and photographed under an inverted microscope (Eclipse Ti, Nikon) in five fields of view. The number and area of liver nodules were calculated to detect cell metastatic ability in vivo.

Dual-Luciferase Reporter Gene Assay

StarBase (http://starbase.sysu.edu.cn/), TargetScan (http://www.targetscan.org/), miRDB (http://www.mirdb.org), miRwalk (http://mirwalk.umm.uni-heidelberg.de/), miRBase (http://www.mirbase.org) and miRanda (http://www.miranda.org.uk/) were applied to predict the binding sites between mRNA and miRNA. The constructed wild-type and mutant sequences, with miRNA mimics and NC, were inserted into a psi-CHECK2 vector and then co-transfected into 293T cells. Lipofectamine 3000 was utilized in co-transfection. 293T cells were seeded in 96-well plates at 1 × 10^4 cells/wells, and the fluorescence intensity was detected by a Dual-Luciferase reporter assay system (Promega, Madison, WI, USA) 48 hours post-transfection. The fluorescence intensity was expressed as firefly luciferase/renilla luciferase.

Western Blot Assay

Lysed by radioimmunoprecipitation assay buffer (Takara, Tokyo, Japan), the cell protein (30 μg) was isolated by sodium dodecyl sulfate-polyacrylamide gel electrophoresis, transferred to a polyvinylidene fluoride (PVDF) membrane and blocked with 1% skim milk powder. After being probed with the primary antibody, the PVDF membrane was re-probed with the secondary antibody, followed by development with enhanced chemiluminescent and exposure under the Chemiluminescence Imaging System (Bio-Rad, Hercules, CA, USA). ImageJ software was utilized for evaluating the optical density of protein bands. The primary antibodies included TIMP3 (ab276134, 1:1000, Abcam, Cambridge, UK), PI3K (#4249, 1:1000, Cell Signaling Technologies, Beverly, MA, USA), AKT (#9272, 1:1000, Cell Signaling Technologies), GAPDH (#5174, 1:800, Cell Signaling Technologies), p-PI3K (1:100, Sigma-Aldrich), p-AKT (ab38449, 1:800, Abcam), and goat anti-rabbit secondary antibody (ab205718, 1:5000, Abcam).

Statistical Analysis

SPSS 22.0 (IBM, NY, USA) statistical software was utilized for data analysis. Data were normally distributed which was detected by Kolmogorov–Smirnov test. Data

were expressed as mean ± standard deviation. The *t*-test was applied for statistical significance between the two groups. One-way or two-way analysis of variance (ANOVA) was adopted for statistical significance among multiple groups, followed by Tukey's multiple comparisons test. Kaplan-Meier analysis was applied to calculate the survival curve. $P < 0.05$ suggested statistical significance.

Results

MiR-21 is Up-Regulated in CSCC Tissues and Cells

In order to find the miRNA highly expressed in CSCC, miRNA microarray analysis was performed on tumor tissues and adjacent tissues of three randomly selected CSCC patients. It was manifested that eight miRNAs were up-regulated in tumor tissues, among which miR-21 was the most up-regulated one (Figure 1A). Further detection of miR-21 expression in all CSCC patients was carried out, and the results exhibited that miR-21 was up-regulated in CSCC patients (Figure 1B). Survival analysis revealed that patients with higher miR-21 had a lower survival rate and shorter survival time than those with lower miR-21 (Figure 1C). miR-21 expression in HSC-1, A431 and HaCaT cells was measured, with the results indicating that miR-21 was elevated in HSC-1 and A431 cells versus HaCaT cells (Figure 1D).

Down-Regulating miR-21 Reverts the Malignant Phenotype of CSCC Cells

Afterwards, miR-21 down-regulation was introduced in HSC-1 and A431 cells. Three miR-21 inhibitor fragments were synthesized for transfection. RT-qPCR implied that miR-21 inhibitor#1 demonstrated the highest efficiency, which was selected for the subsequent analysis (Figure 2A). After miR-21 knockdown in HSC-1 and A431 cells, cells were cultured for the same period under the same conditions. Cultured to the 7th day, the colony formation of cells with poorly expressed miR-21 was diminished (Figure 2B). EdU assay demonstrated that EdU-positive rate reduced in cells with poor miR-21 expression (Figure 2C). Scratch test observed that after 24 hours of incubation, the wound healing rate of cells with depleted miR-21 was slower (Figure 2D). Seeded in the Transwell chamber and cultured for 24 hours, it was depicted that cells with down-regulated

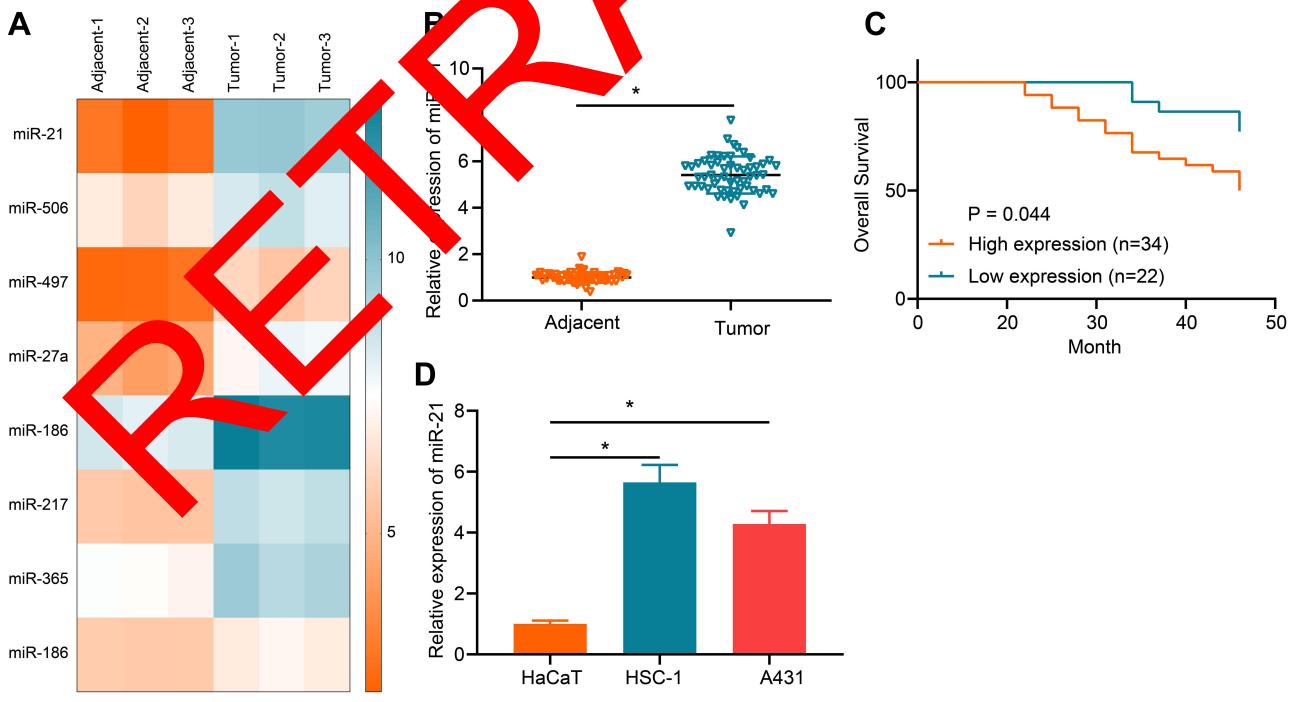

Figure 1 MiR-21 is up-regulated in CSCC tissues and cells. (**A**) Microarray-based analysis of up-regulated miRNAs in tumor tissues (n =3); (**B**) RT-qPCR of miR-21 expression in tumor tissues and adjacent tissues (n = 56, *$P < 0.05$ according to the paired *t*-test); (**C**) Overall survival of CSCC patients (cut-off value of 4.37) with miR-21 high expression and low expression (n = 56, according to Kaplan-Meier analysis); (**D**) RT-qPCR of miR-21 expression in HaCaT, HSC-1 and A431 cells (*$P < 0.05$ according to the one-way ANOVA).

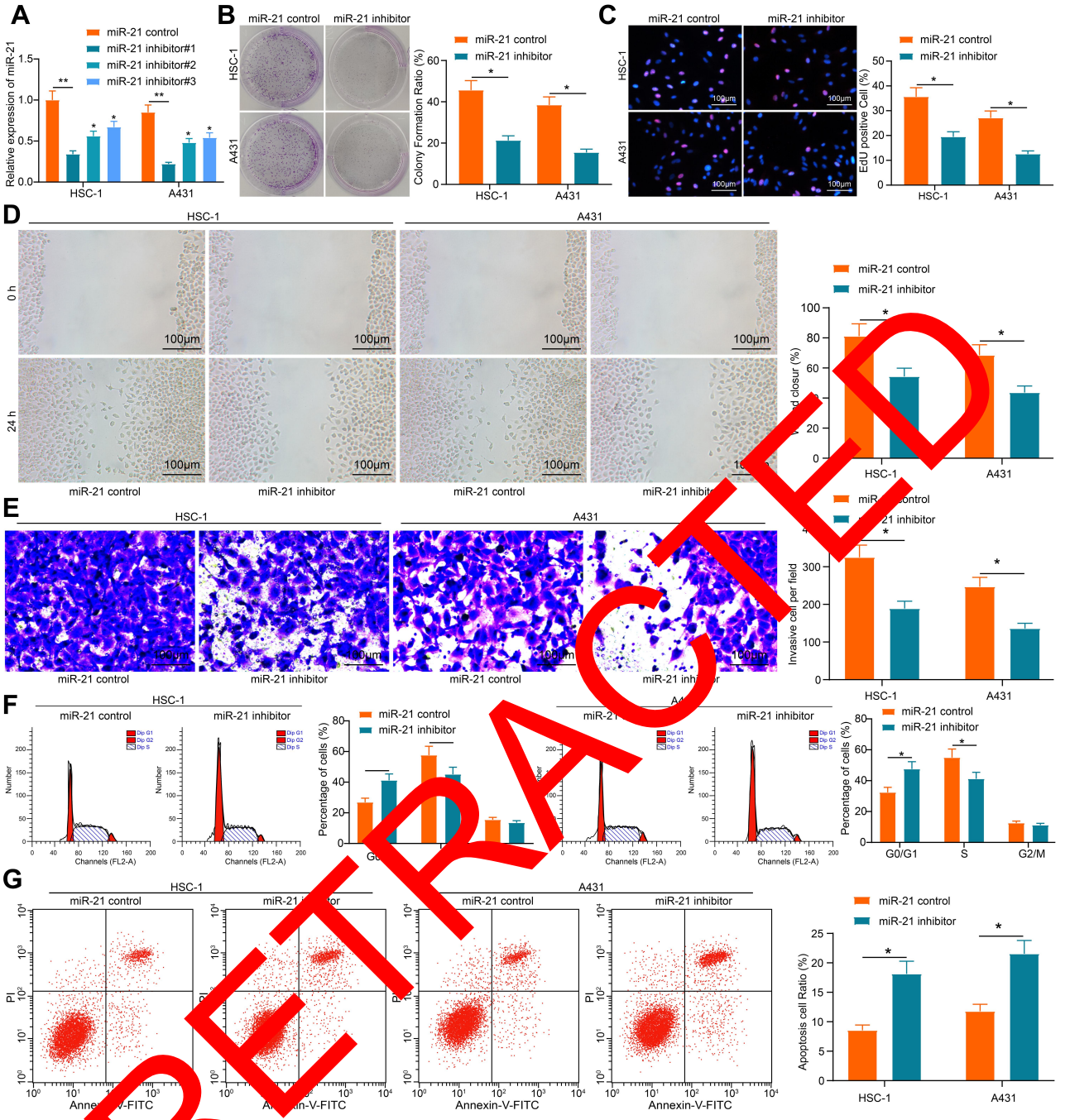

Figure 2 Down-regulation of miR-21 suppresses malignant aggressiveness of CSCC cells. (**A**) RT-qPCR of miR-21 expression in HSC-1 and A431 cells transfected with miR-21 inhibitor (*P < 0.05, **P < 0.01 according to the two-way ANOVA); (**B**) Colony formation assay of cell colony-forming ability (*P < 0.05 according to the two-way ANOVA); (**C**) EdU assay of cell proliferation (*P < 0.05 according to the two-way ANOVA); (**D**) Scratch test of cell migration ability (*P < 0.05 according to the two-way ANOVA); (**E**) Transwell assay of cell invasion ability (*P < 0.05 according to the two-way ANOVA); (**F**) Flow cytometry of cell cycle distribution (*P < 0.05 according to the two-way ANOVA); (**G**) Flow cytometry of cell apoptosis (*P < 0.05 according to the two-way ANOVA); The results represent the average of three experiments.

miR-21 in the basolateral chamber were decreased, indicating impaired invasion ability (Figure 2E). Flow cytometry of cell cycle distribution and apoptosis implied that miR-21 down-regulation arrested most cells in the G0/G1 phase and reduced cells in the S phase (Figure 2F), but also increased apoptotic cells and impaired cell viability (Figure 2G). It could be summarized that miR-21 down-regulation partially prevented CSCC cells from proliferating, invading and migrating and advanced apoptosis.

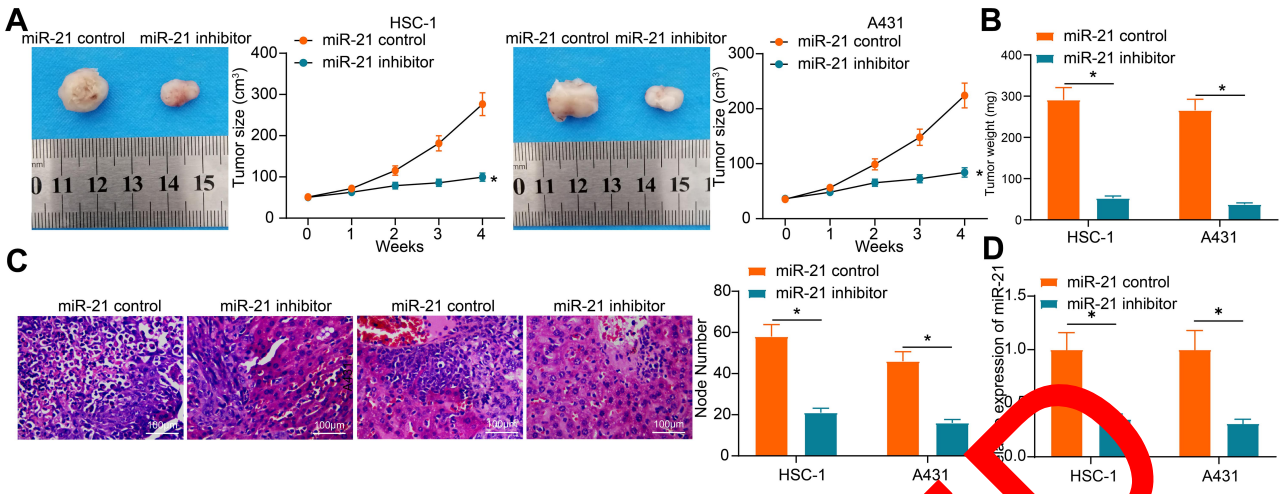

Figure 3 Down-regulating miR-21 retards CSCC tumor formation and metastasis in mice. (**A**) Xenografted tumor volume changes (*P < 0.05 according to the two-way ANOVA); (**B**) Xenografted tumor weight changes (*P < 0.05 according to the two-way ANOVA); (**C**) HE staining of area and number of liver nodules in mice (*P < 0.05 according to the two-way ANOVA); (**D**) RT-qPCR of miR-21 expression in mouse tumor tissues (*P < 0.05 according to the two-way ANOVA); The results represent the average of three experiments.

Down-Regulating miR-21 Retards CSCC Tumor Formation and Liver Metastasis in Mice

Mice were injected with cells transfected with miR-21 inhibitor or its NC, and tumor volume was measured every 7 days. It was outlined that the tumor grew slowly in mice injected with miR-21 inhibitor-transfected cell (Figure 3A). About 28 days later, the tumors were harvested from mice and weighed, and depleted miR-21 reduced tumor weight (Figure 3B). After intravenous injection of cells with miR-21 inhibitor, the livers of mice on the 30th day were stained and observed, with the findings picturing that miR-21 depletion reduced the number of liver nodules (Figure 3C). The expression of miR-21 in mouse xenograft tumors was examined and found to be significantly reduced in the tumors harboring miR-21 inhibitor (Figure 3D), indicating that downregulation of miR-21 inhibited CSCC growth and metastasis in vivo.

TIMP3 is Targeted by miR-21

It was predicted by StarBase, TargetScan, miRDB, miRwalk, miRBase and miRanda that TIMP3 was targeted by miR-21 (Figure 4A). Dual-luciferase report gene assay was adopted to validate the targeting relationship between TIMP3 and miR-21, and the results elucidated that the fluorescence intensity of cells co-transfected with miR-21 inhibitor and TIMP3-WT was enhanced (Figure 4B). Detection of TIMP3 expression in tumor tissues and adjacent tissues revealed that TIMP3 was down-regulated in CSCC patients (Figure 4C). Correlation analysis of miR-21 and TIMP3 expression in CSCC tissues of patients suggested a negative connection (Figure 4D). In terms of the linkage between TIMP3 expression and overall survival of CSCC patients, the results illustrated that TIMP3 expression at a high level contributed to a higher survival rate and longer survival time than patients with TIMP3 at a low expression (Figure 4E). TIMP3 down-regulation was administrated into cells, and TIMP3 expression was the lowest in the second fragment (Figure 4F). TIMP3 down-regulation resulted in enhanced cell invasion and migration abilities in Transwell assays (Figure 4G). Furthermore, the poor expression of TIMP3 increased liver nodules number and enlarged liver nodules area (Figure 4H).

Silencing of TIMP3 Reverses the Effects of miR-21 Down-Regulation on CSCC

CSCC cells were transfected with miR-21 inhibitor alone or with TIMP3 si. To verify the transfection efficiency of TIMP3 si and its correlation with miR-21, we examined the protein expression of TIMP3 in cells after transfection. The results of Western blot revealed that miR-21 inhibitor significantly increased TIMP3 protein expression in cells, while co-transfection of TIMP3 si effectively suppressed its expression (Figure 5A). TIMP3 down-regulation antagonized the inhibitory effects of miR-21 down-regulation on colony-forming ability, migration distance and invasion and the promoting effect on cell apoptosis (Figure 5B–E). TIMP3 down-regulation followed by miR-21 depletion increased liver nodules and promoted metastasis in mice (Figure 5F).

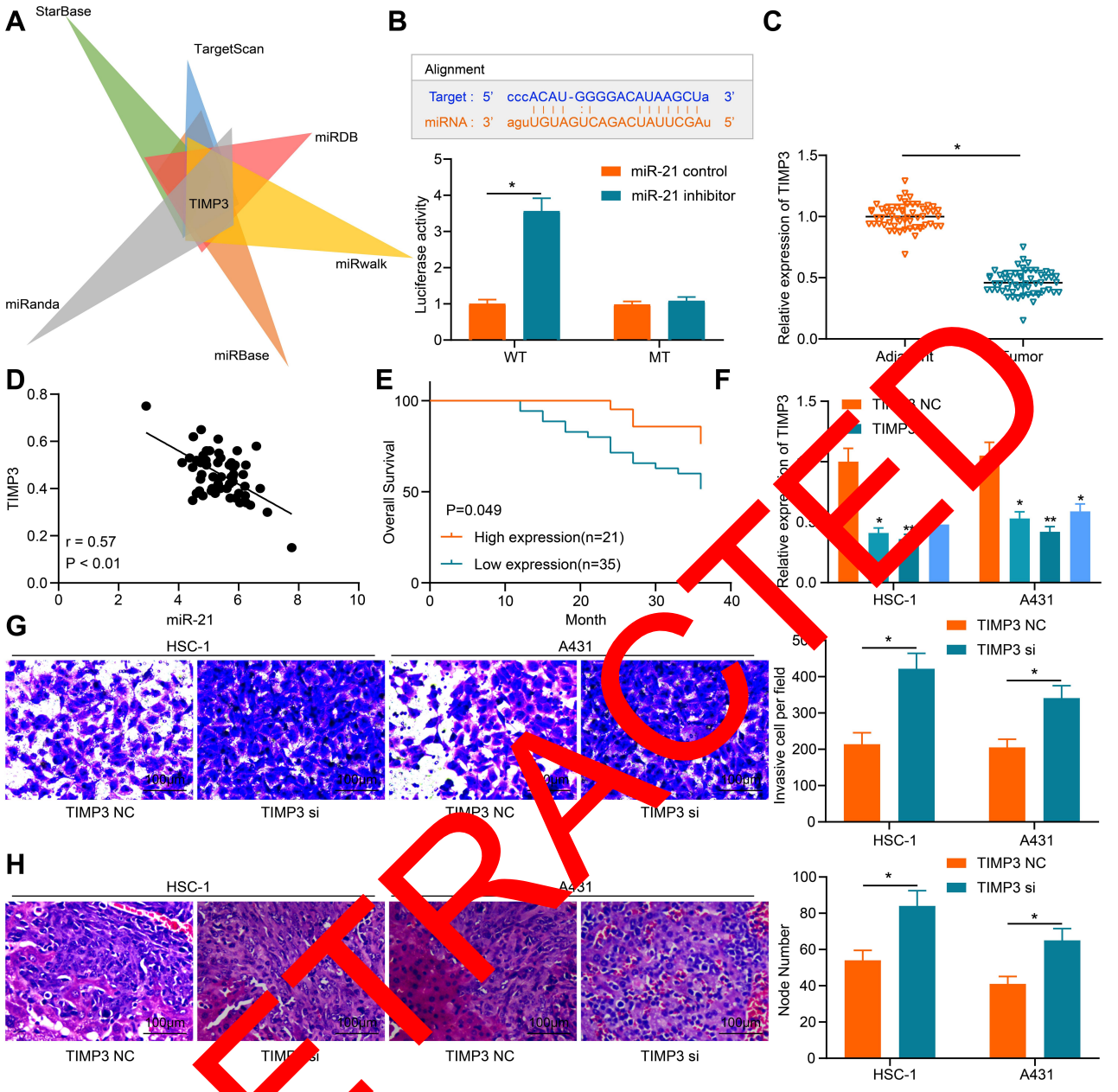

Figure 4 TIMP3 is ta[illegible]ed b[illegible]iR-21. ([illegible] Venn [illegible]gram to screen mRNA targeted by miR-21; (**B**) Dual-luciferase reporter gene assay of the targeting relationship between miR-21 and TIMP3 [illegible] $P < 0.05$ [illegible]cording to [illegible]wo-way ANOVA); (**C**) RT-qPCR of TIMP3 expression in tumor tissues and adjacent tissues of CSCC patients (*$P < 0.05$ according to th[illegible]aired *t*-tes[illegible] (**D**) Correlation analysis between miR-21 and TIMP3 in tumor tissues; (**E**) Overall survival of CSCC patients (cut-off value of 0.42) with TIMP3 high expre[illegible]n an[illegible]w exp[illegible] (n = 56, *$P < 0.05$ according to Kaplan-Meier analysis); (**F**) RT-qPCR of TIMP3 expression in cells transfected with TIMP3 si (*$P < 0.05$, **$P < 0.01$ acc[illegible], to the two-way ANOVA); (**G**) Transwell assay of cell invasion ability (*$P < 0.05$ according to the two-way ANOVA); (**H**) HE staining of area and number of liver nodules [illegible]mice (*$P < 0.05$ according to the two-way ANOVA); The results represent the average of three experiments.

Down-Regulating miR-21 Impairs the PI3K/AKT Signaling Pathway Activation in CSCC

The PI3K/AKT pathway has been evidenced to be involved in the pathogenesis of CSCC.[12] Notably, another study has proved that the PI3K/AKT pathway serves as a mediator in CSCC cell growth and development.[13] Therefore, the phosphorylation levels of PI3K and AKT in CSCC cells were examined, and the results suggested that PI3K/AKT pathway was activated (Figure 6A). Due to the higher activation of PI3K/AKT pathway in HSC-1 cells, HSC-1 cells transfected with miR-21 inhibitor were utilized for subsequent Western blot for PI3K/AKT pathway activity assessment. It was demonstrated that miR-21

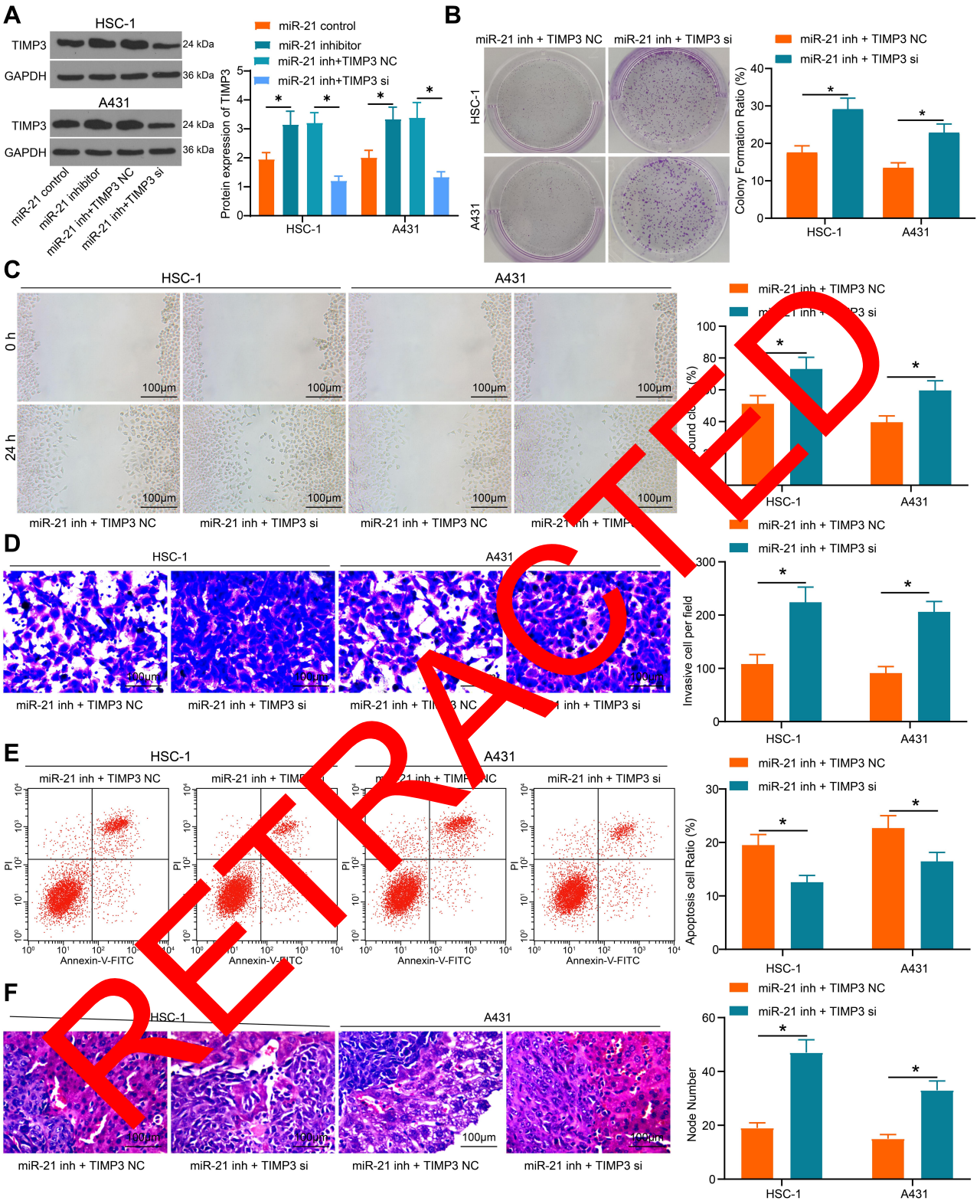

Figure 5 Silencing of TIMP3 reverses the effects of miR-21 down-regulation on CSCC. (**A**) TIMP3 expression in cells after co-transfection determined by Western blot (*P < 0.05 according to the two-way ANOVA); (**B**) Colony formation assay of cell colony-forming ability (*P < 0.05 according to the two-way ANOVA); (**C**) Scratch test of cell invasion ability (*P < 0.05 according to the two-way ANOVA); (**D**) Transwell assay of cell migration ability (*P < 0.05 according to the two-way ANOVA); (**E**) Flow cytometry of cell apoptosis (*P < 0.05 according to the two-way ANOVA); (**F**) HE staining of area and number of liver nodules in mice (*P < 0.05 according to the two-way ANOVA); The results represent the average of three experiments.

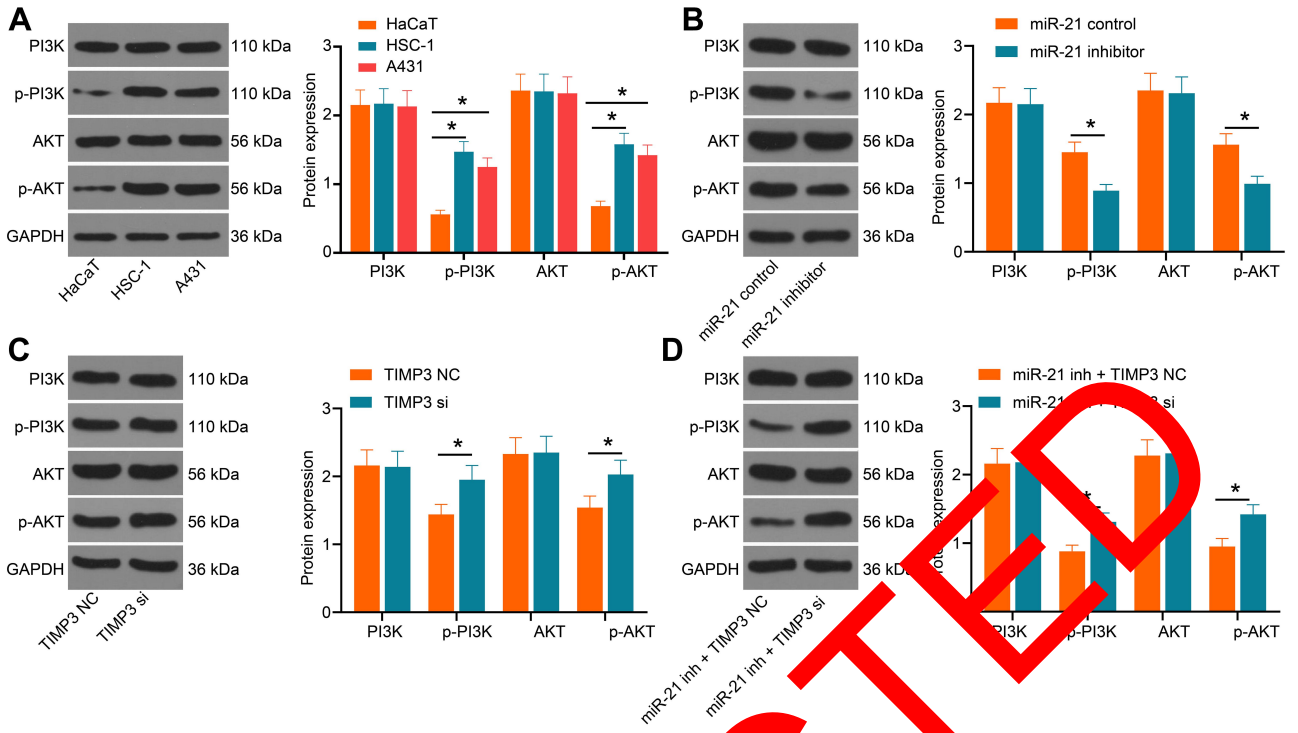

Figure 6 Down-regulating miR-21 inhibits PI3K/AKT signaling pathway activation via mediating TIMP3 in CSCC. (**A**) Expression levels and phosphorylation levels of PI3K and AKT in CSCC cells; (**B**) Expression levels and phosphorylation levels of PI3K and AKT in CSCC cells upon miR-21 inhibitor treatment; (**C**) Expression levels and phosphorylation levels of PI3K and AKT in CSCC cells upon TIMP3 si treatment; (**D**) Expression levels and phosphorylation levels of PI3K and AKT in CSCC cells with treatment of miR-21 inhibitor and TIMP3 si; *$P < 0.05$ according to the two-way ANOVA. The results represent the average of three experiments.

suppression hindered the activation of PI3K/AKT pathway. It indicated that miR-21 affected PI3K/AKT pathway activation, while changes in the PI3K/AKT pathway activity are also responsible for the changes in CSCC cell activity caused by miR-21 down-regulation (Figure 6B). In cells transfected with TIMP3 si, the phosphorylation levels of PI3K and AKT were increased, suggesting that the effect of TIMP3 on cell activity is caused by impairment of the PI3K/AKT pathway (Figure 6C). Also, PI3K/AKT pathway activation was reinforced after co-transfected with miR-21 inhibitor and TIMP3 si (Figure 6D), which further proved the targeting relationship between miR-21 and TIMP3. The above results indicated that miR-21 mediated PI3K/AKT pathway by regulating TIMP3 in CSCC.

Discussion

Ranked as the most prevalent cancers among the white populations, CSCC imposes threatens on human health with metastatic potentials.[16] Furthermore, miRNAs are participated in modulating the expression of cancer-related genes by enhancing the initiation, development, invasiveness, and aggressiveness of CSCC, making them potential prognostic biomarkers and therapeutic candidates in CSCC target therapy.[17] Enlightened by the previous studies, which have validated the potent roles of miR-21 in CSCC, this work is launched with the results concluding that miR-21 overexpression facilitated the development of CSCC through down-regulating TIMP3 and potentiating PI3K/AKT pathway activation.

Initially, determinations of miR-21 in clinical CSCC tissues were implemented with the results stratifying that miR-21 expression was elevated in CSCC tissues and cells, and miR-21 expression was negatively associated with the overall survival of CSCC patients. Then, miR-21 down-regulation assays were performed on CSCC cells, and it was manifested that miR-21 depletion reverted the malignant phenotype of CSCC cells. For further validation, cell transfected with miR-21 inhibitor was injected into mice, and the treated mice were featured by suppressed tumor growth and liver metastasis. As depicted in former studies, it is supportive that miR-21 expression is up-regulated in CSCC.[8,9,18] Actually, miR-21 up-regulation is documented to promote cell migration in vitro and metastasis in vivo in melanoma.[19] Moreover, it is surveyed that miR-21 reaches a high level in primary

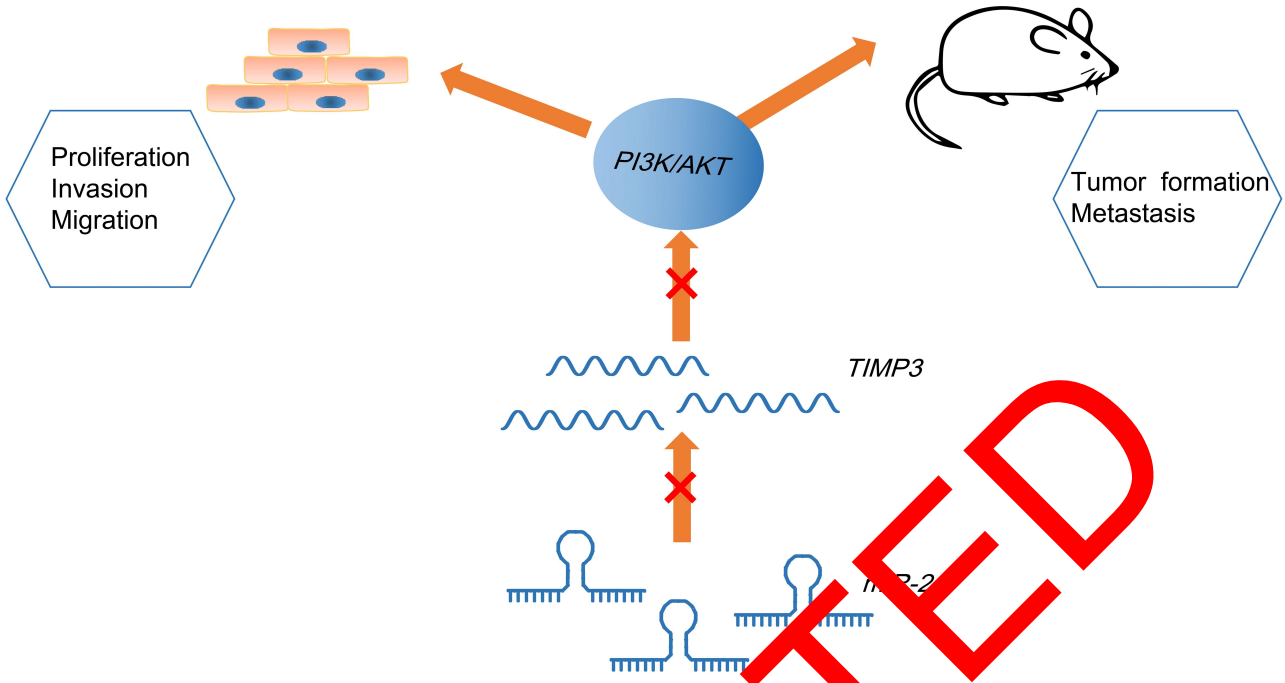

Figure 7 Mechanism diagram suggests that miR-21 targets TIMP3 to activate PI3K/AKT pathway to promote biological activities of CSCC cells and tumor formation and liver metastases in mice.

melanoma tissues and miR-21 elimination induces melanoma cell apoptosis.[20] Intriguingly, overexpressed miR-21 is connected with advanced clinical stage and unsatisfactory 5-year overall survival, and depleting miR-21 is beneficial for apoptosis and chemo- or radiosensitivity in human cutaneous malignant melanoma.[21] Echoed with the findings in this work, miR-21 expression is raised in breast cancer tissues, which is connected with dismal survival rate.[22] All these data suggest that miR-21 plays an oncogenic role in human diseases.

Followed by that online websites and dual-luciferase reporter gene assays have predicted and verified that miR-21 targeted and negatively connected with TIMP3. Also, TIMP3 was down-regulated in clinical CSCC tissues, which also was linked to the unsatisfactory survival of patients. TIMP3 down-regulation assays were conducted in cells and mice, and the results demonstrated that TIMP3 knockdown promoted CSCC cell invasion and liver metastasis in mice. Exactly, there are studies identifying the targeting connection between miR-21 and TIMP3[23,24] which are supportive to our finding. Mechanistically, TIMP3 elevation by down-regulating miR-21 accredits to decreased colon cancer cell invasion and metastasis in vitro and in vivo.[25] A reduction can be seen in TIMP3 expression in melanoma which is related to overall and disease-free survival, and its restoration sets obstructions in the way of melanoma cell invasion and migration.[12] Besides, conclusion drawn from a previous study has suggested that TIMP3 inhibition induced by elevated miR-21 results in increments in the invasiveness of melanoma cells.[13] Briefly, the listed studies have confirmed the results concluded in this work.

Subsequently, for a thorough comprehension of the involvement of miR-21/TIMP3 axis in CSCC, the extent of PI3K and AKT phosphorylation were detected. The findings elucidated that miR-21 inhibition disrupted the PI3K/AKT pathway activation, as evidenced by the reduced extent of PI3K and AKT phosphorylation, which was antagonized by down-regulating TIMP3, indicating that miR-21 targeted TIMP3 to mediate the PI3K/AKT pathway activation. The activated PI3K/AKT pathway has been mentioned in skin cancer carcinogenesis,[26] and the PI3K/AKT pathway deficit can partially attenuate melanoma progression.[27] Moreover, the PI3K/AKT/mTOR pathway was displayed by Nardo et al to play an indispensable role in the pathogenesis of CSCC.[14] A recent study indicated that miR-21 directly targets and inhibits the expression of PTEN (a negative modulator of the PI3K/AKT pathway), and miR-21 inhibition upregulated PTEN expression but impaired the PI3K/AKT pathway, thereby elevating liver cancer cell apoptosis.[28] Furthermore, miR-21 down-regulation causes an

impairment in PI3K/AKT pathway activation in Burkitt's lymphoma.[29] Also, PI3K/AKT pathway activation is in part suppressed by up-regulating TIMP3 in oral squamous cell carcinoma.[30] Anyway, the aforementioned research presentations are echoed with the discoveries in this work.

Conclusion

In summary, this work has elaborated that restoring of miR-21 or silencing of TIMP3 deteriorates CSCC by activating the PI3K/AKT pathway (Figure 7), which replenishes the exited knowledge about CSCC-oriented mechanism. However, limited by the relatively small experimental scale, a large cohort of researches are in need of further confirmation of the results concluded in this study.

Funding

There is no funding to report.

Disclosure

The authors declare that they have no competing interests.

References

1. Fernandez-Guarino M, Zamorano Leon JJ, Lopez Farre AJ, et al. Cytoplasmic increase in Hsp70 protein: a potential new biomarker of early infiltration of cutaneous squamous cell carcinoma arising from actinic keratosis. *Cancers (Basel)*. 2020;12(5):1151. doi:10.3390/cancers12051151
2. Egolf S, Capell BC. LSD1: a viable therapeutic target in cutaneous squamous cell carcinoma? *Expert Opin Ther Targets*. 2020;[illegible]
3. Maubec E. Update of the management of cutaneous squamous-cell carcinoma. *Acta Derm Venereol*. 2020;100(adv00143. doi:10.2340/00015555-3498
4. Zhao G, Kim KY, Zheng Z, et al. AXIN2 and SNAIL expression predict the risk of recurrence in cutaneous squamous cell carcinoma after Mohs micrographic surgery. *Oncol Lett*. 2020;[illegible](3):2133–2140. doi:10.3892/ol.2020.1132
5. Neagu M, Constantin C, Cretoiu SM, Zurac S. miRNAs in the diagnosis and prognosis of skin cancer. *Front Cell Dev Biol*. 2020;8:71. doi:10.[illegible]/fcell.2020.00071
6. Konicke K, Lopez-Luna A, Munoz-Carrillo JL, et al. The microRNA landscape of cutaneous squamous cell carcinoma. *Drug Discov Today*. 2018;[illegible](4):[illegible]10.1016/j.drudis.2018.01.023
7. Darido C, Georgy SR, Cullinane C, et al. Stage-dependent therapeutic efficacy in PI3K/mTOR-driven squamous cell carcinoma of the skin. *Cell Death Dis*. 2018;25(6):1146–1159. doi:10.1038/s41418-017-0032-0
8. Stojadinovic O, Ramirez H, Pastar I, et al. MiR-21 and miR-205 are induced in invasive cutaneous squamous cell carcinomas. *Arch Dermatol Res*. 2017;309(2):133–139. doi:10.1007/s00403-016-1705-0
9. Bruegger C, Kempf W, Spoerri I, Arnold AW, Itin PH, Burger B. MicroRNA expression differs in cutaneous squamous cell carcinomas and healthy skin of immunocompetent individuals. *Exp Dermatol*. 2013;22(6):426–428. doi:10.1111/exd.12153
10. Gao Y, Zou T, Liang W, Zhang Z, Qie M. Long non-coding RNA HAND2-AS1 delays cervical cancer progression via its regulation on the microRNA-21-5p/TIMP3/VEGFA axis. *Cancer Gene Ther*. 2020. doi:10.1038/s41417-020-00243-y
11. Das AM, Koljenovic S, Oude Ophuis CM, et al. Association of TIMP3 expression with vessel density, macrophage infiltration and prognosis in human malignant melanoma. *Eur J Cancer*. 2016;53:135–143. doi:10.1016/j.ejca.2015.09.014
12. Das AM, Bolkestein M, van der Klok T, et al. Tissue inhibitor of metalloproteinase-3 (TIMP3) expression decreases during melanoma progression and inhibits melanoma cell migration. *Eur J Cancer*. 2016;66:34–46. doi:10.1016/j.ejca.2016.06.020
13. Martin Del Campo SE, Latchana N, Levine KM, et al. MiR-21 enhances melanoma invasiveness via inhibition of tissue inhibitor of metalloproteinases 3 expression: in vivo effects of MiR-21 inhibitor. *PLoS One*. 2015;10(1):e0115919. doi:10.1371/journal.pone.0115919
14. Di Nardo L, Pellegrini C, Di Stefani A, et al. Molecular genetics of cutaneous squamous cell carcinoma: prognostic for treatment strategies. *J Eur Acad Dermatol Venereol*. 2019.
15. Ci C, Wu C, Lyu D, et al. Downregulation of kynurenase restrains cutaneous squamous cell carcinoma proliferation and suppresses the PI3K/AKT pathway. *Clin Exp Dermatol*. 2020;[illegible](2):194–201. doi:10.1111/ced.14072
16. Stratigos AJ, Garbe C, Lebbe C, et al. Eurodermoncology interdisciplinary guideline on invasive squamous cell carcinoma of the skin: part 1. epidemiology, diagnostics and prevention. *Eur J Cancer*. 2020.
17. Garofoli M, Colpi[illegible]a M, Guida M, Porcelli L, Azzariti A. The role of non-coding RNAs as prognostic factor, predictor of drug response or resistance and pharmacological targets, in the cutaneous squamous cell carcinoma. *Cancers (Basel)*. 2020;12(9):9. doi:10.3390/cancers12092552
18. Li N, Zhang L, Weisgen F, et al. MicroRNA-125b down-regulates matrix metallopeptidase 13 and inhibits cutaneous squamous cell carcinoma cell proliferation, migration, and invasion. *J Biol Chem*. 2012;287(35):29899–29908. doi:10.1074/jbc.M112.391243
19. Li L, Yuan SM, Yang M, et al. High intensity focused ultrasound inhibits melanoma cell migration and metastasis through attenuating microRNA-21-mediated PTEN suppression. *Oncotarget*. 2016;7(31):50450–50460. doi:10.18632/oncotarget.10433
20. Satzger I, Mattern A, Kuettler U, et al. microRNA-21 is upregulated in malignant melanoma and influences apoptosis of melanocytic cells. *Exp Dermatol*. 2012;21(7):509–514. doi:10.1111/j.1600-0625.2012.01510.x
21. Jiang L, Lv X, Li J, et al. The status of microRNA-21 expression and its clinical significance in human cutaneous malignant melanoma. *Acta Histochem*. 2012;114(6):582–588. doi:10.1016/j.acthis.2011.11.001
22. Wu X. Expressions of miR-21 and miR-210 in breast cancer and their predictive values for prognosis. *Iran J Public Health*. 2020;49(1):21–29.
23. Wang F, Gao X, Zhang R, Zhao P, Sun Y, LncRNA LC. TUG1 ameliorates diabetic nephropathy by inhibiting miR-21 to promote TIMP3-expression. *Int J Clin Exp Pathol*. 2019;12(3):717–729.
24. Wang Y, Yang LZ, Yang DG, et al. MiR-21 antagomir improves insulin resistance and lipid metabolism disorder in streptozotocin-induced type 2 diabetes mellitus rats. *Ann Palliat Med*. 2020;9(2):394–404. doi:10.21037/apm.2020.02.28
25. Wang J, Lin Y, Jiang T, et al. Up-regulation of TIMP-3 and RECK decrease the invasion and metastasis ability of colon cancer. *Arab J Gastroenterol*. 2019;20(3):127–134. doi:10.1016/j.ajg.2019.07.003
26. Li X, Zuo C, Wu M, Zhang Z. Linc-ROR promotes arsenite-transformed keratinocyte proliferation by inhibiting P53 activity. *Metallomics*. 2020;12(6):963–973. doi:10.1039/D0MT00076K
27. Ning N, Liu S, Liu X, et al. Curcumol inhibits the proliferation and metastasis of melanoma via the miR-152-3p/PI3K/AKT and ERK/NF-kappaB signaling pathways. *J Cancer*. 2020;11(7):1679–1692. doi:10.7150/jca.38624

28. He JQ, Zheng MX, Ying HZ, et al. PRP1, a heteropolysaccharide from platycodonis radix, induced apoptosis of HepG2 cells via regulating miR-21-mediated PI3K/AKT pathway. *Int J Biol Macromol*. 2020;158:542–551. doi:10.1016/j.ijbiomac.2020.04.193
29. Han B, Wang S, Zhao H. MicroRNA-21 and microRNA-155 promote the progression of Burkitt's lymphoma by the PI3K/AKT signaling pathway. *Int J Clin Exp Pathol*. 2020;13(1):89–98.
30. Cheng Z, Xing D. Ginsenoside Rg3 inhibits growth and epithelial-mesenchymal transition of human oral squamous carcinoma cells by down-regulating miR-221. *Eur J Pharmacol*. 2019;853:353–363. doi:10.1016/j.ejphar.2019.03.040